Supporting Information

Spectroscopic X-ray Diffraction for Micro-focus Inspection of Li-Ion Batteries

Haruno Murayama[1], Koji Kitada[1], Katsutoshi Fukuda[1], Akio Mitsui[1], Koji Ohara[1], Hajime Arai[1], Yoshiharu Uchimoto[2], Zempachi Ogumi[1] & Eiichiro Matsubara[3]

[1]*Office of Society-Academia Collaboration for Innovation, Kyoto University, Uji, Kyoto 611-0011, Japan*

[2]*Graduate School of Human and Environmental Studies, Kyoto University, Sakyo-ku, Kyoto 606-8501, Japan*

[3]*Department of Materials Science and Engineering, Kyoto University, Sakyo-ku, Kyoto 606-8501, Japan*

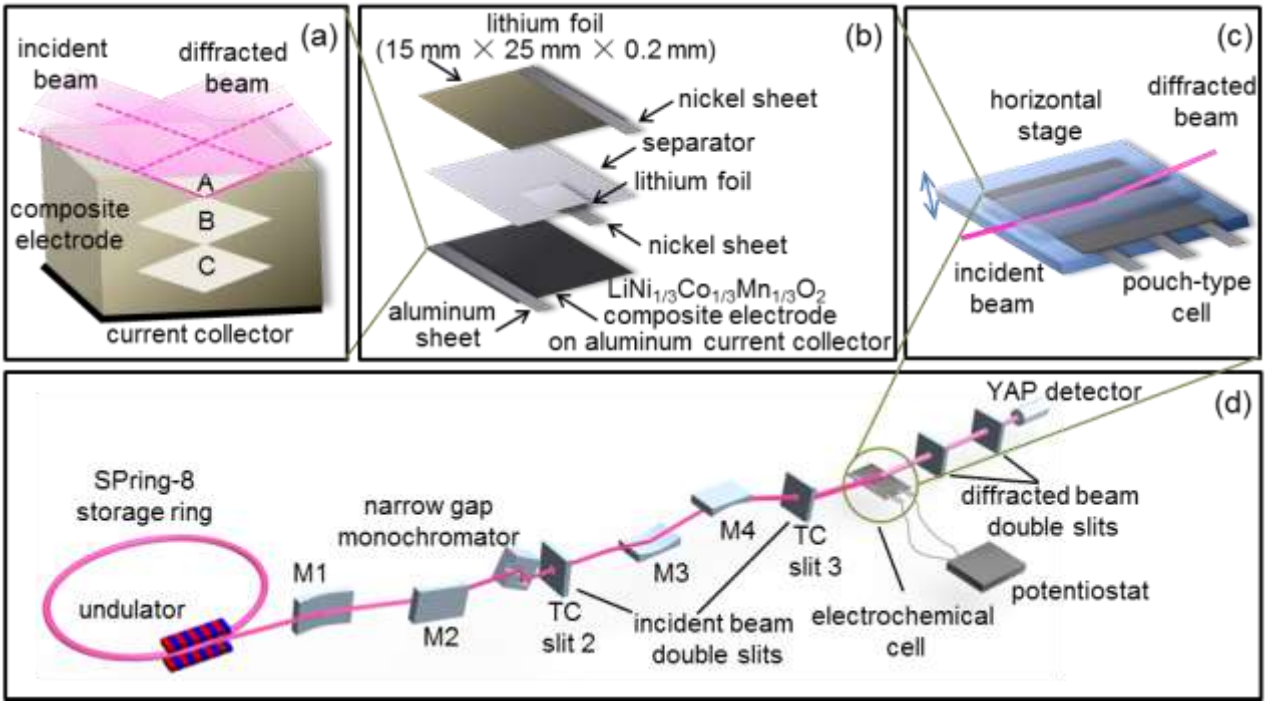

Figure S1. (a) Schematic view of the lozenge-shape probe in the cross section of the composite electrode with the observed positions shown in fig. 3. (b) Configuration of components in the aluminum pouch-type cell. (c) Sketch of setup of the aluminum pouch-type cell for the energy-scanning confocal XRD measurements. Those components are sealed in a laminated aluminum film bag. (d) Schematic layout of the energy-scanning confocal XRD equipment on BL28XU at SPring-8.

S2. Additional explanation of the equations.

Eq 2 is formulated based on a geometric layout shown in Figure S2a and is deduced as follows:

$$H = \frac{gap}{\sin\theta_m} \times \sin 2\theta_m$$

$$= gap \times \frac{2 \sin\theta_m \cos\theta_m}{\sin\theta_m}$$

$$\therefore H = 2 \times gap \times \cos\theta_m$$

Eq 3 is formulated based on a geometric layout shown in Figure S2b and is deduced as follows:

$$h = 2 \times \frac{w}{\sin 2\theta} \times \sin\frac{2\theta}{2}$$

$$= 2 \times \frac{w}{2 \sin\frac{2\theta}{2} \cos\frac{2\theta}{2}} \times \sin\frac{2\theta}{2}$$

$$\therefore h = w/\cos(2\theta/2)$$

Eq 4 is deduced as follows:

$$2\, d_{hkl} \sin\theta = \lambda$$

$$= 2\, d_{Si111} \sin\theta_m$$

$$\therefore d_{hkl} = d_{Si111} \sin\theta_m / \sin\theta$$

Figure S2. Geometric layouts for (a) X-ray beam path through channel-cut monochromator and (b) lozenge-shaped area of confocal point created by incident and receiving slits.

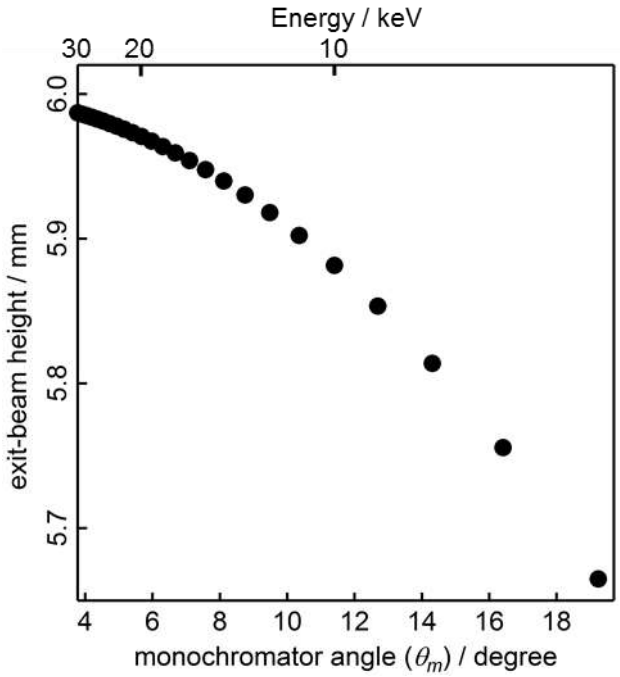

Figure S3. Estimated changes in the exit-beam height from the servomotor-driven compact monochromator with a Si_{111} channel-cut crystal and a 3-mm gap calculated using eq 2. The exit-beam heights are plotted at 1 keV intervals between 6 and 30 keV.

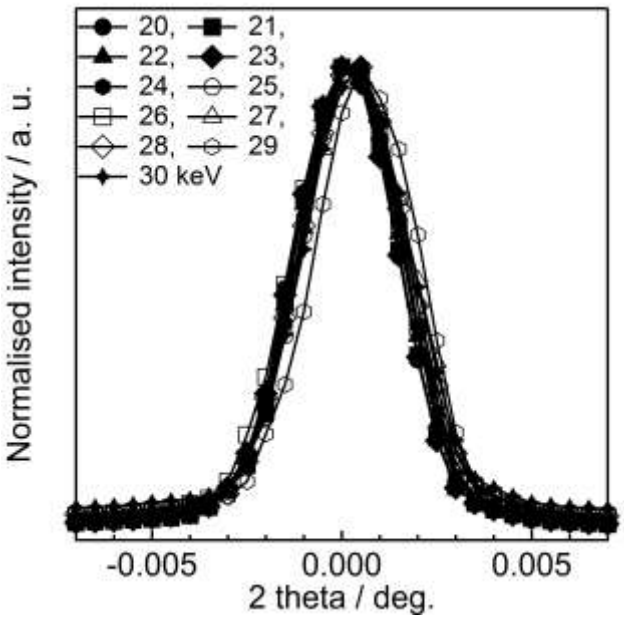

Figure S4. Intensity profiles of the direct beams through the incident and detecting slits, which were set at a height of 50 μm. The intensity profiles were measured using the goniometer equipped with an ion-chamber on the 2θ arm (the goniometer radius is 1 m) at 1 keV intervals in the energy range between 20 and 30 keV. The peak positions and the full width at half maximums (FWHMs) were obtained by peak fitting using Gaussian profile shape functions. Note that a positional repeatability of the goniometer in terms of 2θ arm's position, less than 0.0001˚, is negligible in this estimation. The average and the standard deviation of the peak positions were 4.5 μrad and 2.8 μrad, respectively. The average and the standard deviation of the FWHMs were 55.9 μrad and 1.7 μrad, respectively. The average of the FWHMs is the angular divergence of the X-ray beam ($\Delta\theta$) in eq 5.

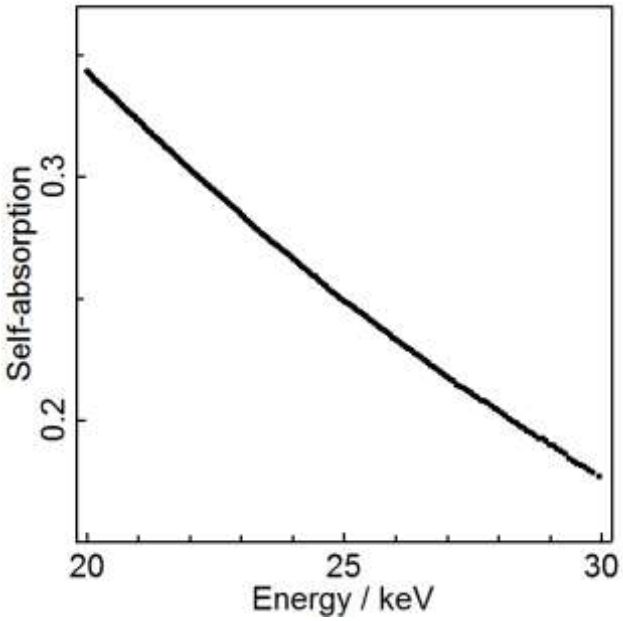

Figure S5. Self-absorption at energy range of 20–30 keV when the incident beam straightly transpierce (*i.e.*, θ = 90 degree) through components of the cell above the aluminum current collector.

Table S1. Δd / ds obtained by the energy-scanning XRD spectrum and the conventional XRD pattern with an angle-scanning range of 2θ from 3.9 to 18.5 degrees at 29 keV as shown in Figure 2

Miller indices	Energy-scanning			Angle-scanning		
	d / Å	Δd / Å	Δd / d	d / Å	Δd / Å	Δd / d
015	1.871	0.0068	0.0036	1.870	0.0062	0.0033
009	1.581	0.0056	0.0035	1.581	0.0074	0.0047
107	1.573	0.0060	0.0038	1.573	0.0059	0.0038
018	1.446	0.0043	0.0030	1.446	0.0050	0.0035
110	1.432	0.0041	0.0029	1.432	0.0043	0.0030
113	1.371	0.0042	0.0031	1.371	0.0042	0.0031